DE GRUYTER OPEN

Int. J. of Applied Mechanics and Engineering, 2016, vol.21, No.2, pp.377-392
DOI: 10.1515/ijame-2016-0023

THERMAL ANALYSIS OF A FULLY WET POROUS RADIAL FIN WITH NATURAL CONVECTION AND RADIATION USING THE SPECTRAL COLLOCATION METHOD

F. KHANI and M.T. DARVISHI
Department of Mathematics, Razi University
Kermanshah 67149, IRAN

R.S..R. GORLA* and B.J. GIREESHA
Department of Mechanical Engineering
Cleveland State University
Cleveland, Ohio-44115, USA
E-mail: r.gorla@csuohio.edu

Heat transfer with natural convection and radiation effect on a fully wet porous radial fin is considered. The radial velocity of the buoyancy driven flow at any radial location is obtained by applying Darcy's law. The obtained non-dimensionalized ordinary differential equation involving three highly nonlinear terms is solved numerically with the spectral collocation method. In this approach, the dimensionless temperature is approximated by Chebyshev polynomials and discretized by Chebyshev-Gausse-Lobatto collocation points. A particular algorithm is used to reduce the nonlinearity of the conservation of energy equation. The present analysis characterizes the effect of ambient temperature in different ways and it provides a better picture regarding the effect of ambient temperature on the thermal performance of the fin. The profiles for temperature distributions and dimensionless base heat flow are obtained for different parameters which influence the heat transfer rate.

Key words: wet porous radial fin, natural convection, radiation, thermal analysis, spectral collocation method.

1. Introduction

An extended surface from an object which is used to increase the rate of heat transfer is called a fin. The heat exchanging devices such as radiators in cars, computers, CPU heatsinks, heat exchangers in power plants, air conditioning, air-cooled aircraft engines, refrigeration devices, and cooling of oil carrying pipe line, etc. have fin applications. Fins are also used in newer technology such as hydrogen fuel cells. Finned surfaces are made by metals including copper, aluminum, iron etc. Aluminum has high thermal conductivity, low weight and resistance to corrosion. The optimization of the size and cost of fins is an important target of fin designers. Some engineering applications require lighter fins with higher rate of heat transfer. In such applications, high thermal conductivity metals are used. Further, the thermal efficiency also depends on the shape of the fin. Therefore, the prime objective of this study is the evaluation of the heat-transfer rate as well as fin efficiency in the presence of a radial fin.

For the last two decades several authors have analyzed the heat transfer analysis of fins. Nguyen and Aziz [1] analyzed the heat transfer rate from convecting-radiating fins for different profile shapes. The optimization of circular fins with variable thermal parameters was studied by Yu and Chen [2], whereas, Abu-Hijleh [3] critically analyzed the enhanced forced convection heat transfer from a cylinder using permeable fins. Kiwan [4] made the thermal analysis of natural convection in porous fins and explained the

* To whom correspondence should be addressed

importance of porous fins in the heat transfer mechanism. The natural convection heat transfer from a thermal heat source located in a vertical plate fin was explained by Mobedi and Sunden [5].

As the efficiency of heat exchange depends on the shape of the fin, Lorenzini and Moretti [6] have discussed the heat removal from Y-shaped fins. Performance and optimization analyses of a constructal T-shaped fin when subject to variable thermal conductivity and convective heat transfer coefficient were made by Kundu and Bhanja [7]. Khani and Aziz [8] studied the thermal analysis of a longitudinal trapezoidal fin with the temperature-dependent thermal conductivity and heat transfer coefficient. Turkyilmazoglu [9] obtained the exact solutions to heat transfer in straight fins of varying exponential shape having temperature dependent properties.

Gorla and Bakier [10] dicussed the thermal analysis of natural convection and radiation in porous fins. Turkyilmazoglu [11] investigated the heat-transfer solutions to radial fins of general profile in closed form. Temperature distribution along a constant cross sectional area fin was obtained by Asadi and Khoshkho [12]. Hatami and Ganj [13] presented a theoretical study on thermal performance of circular convective–radiative porous fins with different section shapes and materials. Later on, Ali and Abubaker [14] discussed the effect of vapour velocity on condensate retention on horizontal pin-fin tubes. Cuce and Cuce [15] conducted a successful application of the homotopy perturbation method for efficiency and effectiveness assessment of longitudinal porous fins. Futher, Turkyilmazoglu [16] analyzed the stretching/shrinking longitudinal fins of rectangular profile and heat transfer.

Motivated by these studies, the main aim of the present paper is to study the thermal analysis of a fully wet porous radial fin with natural convection and radiation. Radial fins are used in numerous applications where porous fins can provide a lighter, cheaper and superior alternative to solid metallic fins. The energy equation governing this problem appears in the form of an ordinary differential equation containing three nonlinear terms. A numerical procedure is adopted to find the solution of the problem for different pertinent parameters. The present formulation characterizes the effect of the ambient temperature in a different manner and provides a better picture of the effect of the ambient temperature on the thermal performance of the fin.

In computational mechanics or numerical simulations, the spectral collocation method (SCM) is one of the spectral methods, which are high order numerical methods and can provide an exponential node convergence rate (in other words, spectral accuracy) [17, 18]. Due to the mathematical simplicity and computational efficiency, the SCM has turned out to be an efficient tool in science and engineering applications, such as computational fluid dynamics [19, 20], magneto-hydrodynamics [21] and thermal radiation heat transfer [22]. To the best of our knowledge, the SCM has not been applied to analyze the heat transfer in a fully wet porous radial fin with natural convection and radiation.

2. Mathematical analysis

Consider a fully wet radial fin of base radius r_b, tip radius r_t and thickness t as illustrated in Fig.1. The base of the fin is maintained at a constant temperature T_b. The tip of the fin is assumed to be adiabatic. The fin is made of a porous material of the effective thermal conductivity k_{eff} and permeability K. The fin is in contact with an ambient fluid which infiltrates through the fin following Darcy's law. The fluid has a specific heat $c_{p,f}$, density ρ_f, kinematic viscosity ν_f, thermal conductivity k_f and coefficient of volumetric expansion β_f. The exposed surfaces (top and bottom) are assumed to be gray with a constant emissivity ε and emit radiation to the ambient fluid (temperature T_b), which also serves as the radiation heat sink.

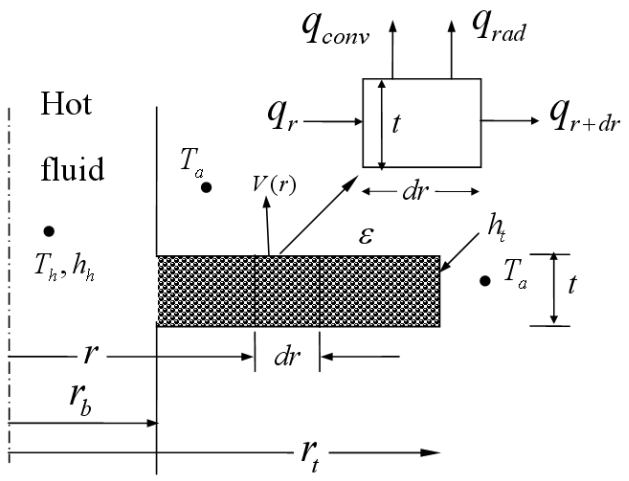

Fig.1. Porous radial fin geometry and energy balance.

Making an energy balance on an element of the fin (Fig.1) of circumference $2\pi r$, thickness t and radial height dr, we get

$$q_r - q_{r+dr} - q_{conv} - q_{rad} = 0 \tag{2.1}$$

where

$$q_r - q_{r+dr} = \frac{d}{dr}\left(k(2\pi rt)\frac{dT}{dr}\right)dr + 2\pi r h_D i_{fg}(1-\varphi)(\varpi - \varpi_a)dr + \\ + h2\pi r dr(1-\varphi)(T - T_a), \tag{2.2}$$

$$q_{rad} = 2\varepsilon\sigma F_{f-a}(2\pi r dr)\left(T^4 - T_a^4\right), \tag{2.3}$$

$$q_{conv} = 2\rho_f \nu(r)(2\pi r dr)c_{p,f}(T - T_a) \tag{2.4}$$

where Eq.(2.2) is based on the application of Fourier's law of heat conduction, Eq.(2.3) is the radiative heat losses from the top and bottom faces of the fin and Eq.(2.4) is the rate of change of enthalpy of the buoyant fluid (infiltrate) passing through the fin. This is the rate at which the energy is removed from the fin by the buoyancy induced flow through the fin. The velocity of the buoyancy driven flow $\nu(r)$ at any radiation location *r* is obtained by applying Darcy's law as follows

$$\nu(r) = \frac{g\beta(T - T_a)}{\nu_f}. \tag{2.5}$$

Substituting Eqs (2.2)-(2.5) into Eq.(2.1) leads to the following nonlinear ordinary differential equation governing the temperature distribution in the fin

$$\frac{1}{r}\frac{d}{dr}\left(r\frac{dT}{dr}\right)-\frac{2\rho_f g\beta_f K}{\nu_f k_{eff} t}\left(T-T_a\right)^2-\frac{2\varepsilon\sigma F_{f-a}}{k_{eff} t}\left(T^4-T_a^4\right)+$$
$$-\frac{2h_D ifg(1-\varphi)(w-w_a)}{K_{eff} t}-\frac{2h(1-\varphi)}{K_{eff} t}\left(T-T_a\right)=0. \tag{2.6}$$

We consider the heat transfer coeeficient, h to vary as given by Torabi and Zhang [23]

$$h=h_a\left[\frac{T-T_a}{T_b-T_a}\right]^p=h_D C_p Le^{2/3}.$$

Let

$$k_{eff}=k_0\left(1+\lambda\left(T-T_a\right)\right)=k_0\left(1+m\left(\theta-\theta_a\right)\right) \tag{2.7}$$

where $k_0=$ effective thermal conductivity at T_a and $m=\lambda T_b$.

The boundary conditions at the fin's base and at its tip may be written as

$$r=r_b,\qquad T=T_b, \tag{2.8}$$

$$r=r_t,\qquad \frac{dT}{dr}=0. \tag{2.9}$$

Introduce the following dimensionless quantities

$$\theta=\frac{T}{T_b},\quad \theta_a=\frac{T_a}{T_b},\quad R=\frac{r}{r_b},\quad K_r=\frac{k_{eff}}{k_f},\quad \mathrm{Da}=\frac{K}{t^2},\quad \mathrm{Gr}=\frac{g\beta_f T_b t^3}{\nu_f^2}, \tag{2.10}$$

$$\mathrm{Pr}=\frac{\nu_f}{\alpha_f},\qquad \mathrm{Ra}=\mathrm{GrPr},\qquad \mathrm{Nc}=\frac{\mathrm{DaRa}}{K_r}\left(\frac{r_b}{t}\right)^2=\frac{\rho_f g K\beta_f c_{p,f} r_b^2 T_b}{\nu_f k_{eff} t},$$

$$Nr=\frac{2\varepsilon\sigma F_{f-a} r_b^2 T_b^3}{k_{eff} t},\qquad m_0=\frac{2r_b^2 h_a(1-\varphi)}{k_0 t},\qquad m_1=\frac{r_b^2\, 2h_a i_{fg}(1-\varphi)b_2}{C_p Le^{2/3} t k_0}, \tag{2.11}$$

$$\varpi-\varpi_a=b_2\left(T-T_a\right),\qquad m_2=m_0+m_1.$$

Rewrite Eqs (2.6)-(2.9) in dimensionless form as follows

$$\frac{1}{R}\frac{d}{dR}\left(R\frac{d\theta}{dR}\right)-\mathrm{Nc}\frac{\left(\theta-\theta_a\right)^2}{1+m\left(\theta-\theta_a\right)}-Nr\frac{\left(\theta^4-\theta_a^4\right)}{1+m\left(\theta-\theta_a\right)}+$$
$$-\left(m_2\right)\frac{\left(\theta-\theta_a\right)^{p+1}}{\left(1+m\left(\theta-\theta_a\right)\right)\left(1-\theta_a\right)^p}=0, \tag{2.12}$$

$$R = 1, \qquad \theta(R) = 1\,, \tag{2.13}$$

$$R = R^*, \quad \frac{d\theta}{dR} = 0. \tag{2. 14}$$

Equation (2.12) is a nonlinear ordinary differential equation. It contains three nonlinear terms, first nonlinearity is due to the natural convective transport of energy by the infiltrate. This energy is the rate at which the enthalpy of the infiltrate increases as it flows through the porous fin. The second nonlinear term is associated with the surface radiative heat transfer from the fin to the ambient fluid which also serves as the radiation sink. The third term is related to moisture in the air with its latent heat of evaporation.

It may be noted that the parameter *Nc* is a combination of Darcy's number Da, Rayleigh number Ra, the thermal conductivity ratio K_r and the ratio of the fin base radius to fin thickness. The parameter *Nr* indicates the role of surface radiation relative to conduction in the fin. The parameter θ_a is the ratio of ambient fluid temperature and the base temperature.

The heat flow through the fin, q, can be found by applying Fourier's law at the base of the fin giving

$$q = -k_0\left(1 + \lambda\left(T_b - T_a\right)\right)\left(2\pi r_b t\right)\frac{dT}{dr}\Big|_{r=r_b}\,, \tag{2.15}$$

or dimensionless form as

$$Q = \frac{q}{2\pi k_0 t T_b} = -\left(1 + m\left(1 - \theta_a\right)\right)\theta'(1)\,. \tag{2.16}$$

In this paper, we solve Eq.(2.12) with boundary conditions (2.13) and (2.14) by a spectral collocation method [17, 18].

3. Numerical method

For convenience of analysis, the energy Eq.(2.12) can be rewritten as

$$\left(1 + m\left(\theta - \theta_a\right)\right)\left(\frac{1}{R}\frac{d\theta}{dR} + \frac{d^2\theta}{dR^2}\right) - \mathrm{Nc}\left(\theta - \theta_a\right)^2 - Nr\left(\theta^4 - \theta_a^4\right) - \left(m_2\right)\frac{\left(\theta - \theta_a\right)^{p+1}}{\left(1 - \theta_a\right)^p} = 0. \tag{3.1}$$

Equation (3.1) is a strong nonlinear ordinary differential equation. Applying the spectral collocation method, Eq.(3.1) can be rearranged as

$$\begin{aligned}
&\left\{\left(1 + m\left(\theta^* - \theta_a\right)\right)\left(\frac{1}{R}\frac{d}{dR} + \frac{d^2}{dR^2}\right) - 2\mathrm{Nc}\theta^* + 2\mathrm{Nc}\theta_a - 2Nr\left(\theta^*\right)^3 + \right.\\
&\left. -\frac{2m_2}{\left(1 - \theta_a\right)^p}\sum_{k=1}^{p+1}\binom{p+1}{k}\left(\theta^*\right)^{k-1}\left(-\theta_a\right)^{p-k+1}\right\}\theta = \mathrm{Nc}\left(\theta_a{}^2 - \left(\theta^*\right)^2\right) + \\
&-Nr\left(\theta_a{}^4 + \left(\theta^*\right)^4\right) - \frac{m_2}{\left(1 - \theta_a\right)^p}\sum_{k=1}^{p+1}\binom{p+1}{k}\left(\theta^*\right)^k\left(-\theta_a\right)^{p-k+1} + \frac{m_2}{\left(1 - \theta_a\right)^p}\left(-\theta_a\right)^{p+1}
\end{aligned} \tag{3.2}$$

where $\binom{p+1}{k} = \frac{(p+1)!}{(p-k+1)!k!}$ and θ^* denote the last iterative value of dimensionless temperature.

The Chebyshev-Gausse-Lobatto collocation points are used for spatial discretization of the dimensionless energy conservation equation

$$\eta_i = -\cos\left(\frac{\pi(i-1)}{N-1}\right), \quad i = 1,2,...,N. \tag{3.3}$$

The above collocation points take values in the interval [-*1*, *1*]. First, the mapping of an arbitrary interval $R \in [R_1, R_2]$ to a standard interval $\eta \in [-1,1]$ is needed to fit the requirement of the Chebyshev polynomial

$$\eta = \frac{2R - (R_2 + R_1)}{R_2 - R_1}, \qquad R = \frac{\eta(R_2 - R_1) + R_2 + R_1}{2}. \tag{3.4}$$

The dimensionless unknown temperature can be approximated by the Chebyshev polynomial as

$$\theta_N(\eta) = \sum_{i=1}^{N} \hat{\theta}_i T_i(\eta) \tag{3.5}$$

where $\theta_N(\eta) \approx \theta(\eta)$ and $\hat{\theta}_i$ are determined by the collocation points η_i, $i = 1,2,..,N$; and the $T_i(\eta)$ is the first kind Chebyshev polynomial. The polynomial of degree N defined by Eq.(3.5) can be the Lagrange interpolation polynomial based on the set $\{\eta_i\}$ like

$$\theta_N(\eta) = \sum_{i=1}^{N} h_i(\eta)\theta(\eta_i) \tag{3.6}$$

where $h_i(\eta)$ is a function of the first order derivative of the Chebyshev polynomial, and its detailed definition can be found in [17,18]

$$h_i(\eta) = \frac{w_i/(\eta - \eta_i)}{\sum_{j=1}^{N} w_j/(\eta - \eta_j)} \tag{3.7}$$

where

$$w_i = (-1)^{i-1}\delta_j, \qquad \delta_j = \begin{cases} 1/2 & j = 1,N \\ 1 & j = 2,3,...,N-1. \end{cases} \tag{3.8}$$

To avoid spectral cofficients solution and fast cosine transformation, we use Eq.(3.6) in Eq.(3.2). One can obtain the spectral discretized algebraic equation

$$\sum_{j=1}^{N} A_{ij}\theta_j = B_i, \qquad i = 1,2,...,N \tag{3.9}$$

where the element of expressions for matrices ***A***, ***B*** are

$$A_{ij}=\begin{cases}\left[1+m\left(\theta_i^*-\theta_a\right)\right]\left\{\dfrac{2}{R_i\left(R^*-1\right)}D_{ij}^{(1)}+\left(\dfrac{2}{R^*-1}\right)^2 D_{ij}^{(2)}\right\}-2\mathrm{Nc}\theta_i^*+2\mathrm{Nc}\theta_a-2Nr\left(\theta_i^*\right)^3+ & i=j\\ -\dfrac{2m_2}{\left(1-\theta_a\right)^p}\displaystyle\sum_{k=1}^{p+1}\binom{p+1}{k}\left(\theta_i^*\right)^{k-1}\left(-\theta_a\right)^{p-k+1} & \\ \left[1+m\left(\theta_i^*-\theta_a\right)\right]\left\{\dfrac{2}{R_i\left(R^*-1\right)}D_{ij}^{(1)}+\left(\dfrac{2}{R^*-1}\right)^2 D_{ij}^{(2)}\right\} & i\neq j\end{cases} \tag{3.10}$$

$$\begin{aligned}B_i=&\ \mathrm{Nc}\left(\theta_a{}^2-\left(\theta_i^*\right)^2\right)-Nr\left(\theta_a{}^4+\left(\theta_i^*\right)^4\right)+\\ &-\frac{m_2}{(1-\theta_a)^p}\sum_{k=1}^{p+1}\binom{p+1}{k}\left(\theta_i^*\right)^k\left(-\theta_a\right)^{p-k+1}+\frac{m_2}{(1-\theta_a)^p}(-\theta_a)^{p+1}\end{aligned} \tag{3.11}$$

where $D_{ij}^{(1)}$ and $D_{ij}^{(2)}$ are entries of the first order and the second order derivative coefficient matrices, respectively. Their detailed computation can be written as [17, 18].

After imposing the Dirichlet and Neumann boundary conditions (Eqs (2.13) and (2.14)), we can write the matrix form of the above Eq.(3.9) as follows

$$\theta_1=1,\qquad \sum_{j=2}^{N}\hat{A}_{ij}\theta_j=\hat{B}_i,\qquad i=2,\ldots,N. \tag{3.12}$$

The implementation of the spectral collocation method for solving the thermal performance of a fully wet porous radial fin with natural convection and radiation can be executed through the following routine:

Step 1. Input the number of collocation points, and compute the coordinate value of nodes, the first and second order derivative matrix.

Step 2. Initialize the value of dimensionless temperature initial θ^* assumptions (zero for example) in all directions except of boundaries.

Step 3. Assemble matrices ***A*** and ***B*** by Eqs (3.10), (3.11).

Step 4. Impose boundary conditions in Eqs (2.13) and (2.14), and compute matrices $\hat{A}$ and $\hat{B}$.

Step 5. Terminate the iteration if the maximum absolute difference of the last and present dimensionless temperature is less than the tolerance (10^{-12} for example), otherwise go back to step 3.

Step 6. Compute the dimensionless temperature and base heat flow.

4. Results and discussion

The thermal analysis of a fully wet porous radial fin with natural convection and radiation is studied numerically. The obtained non-dimensionalized ordinary differential equations involving two nonlinear terms, associated with the buoyancy effects in the fluid and the permeability of the porous medium and with a consequence of radiative cooling at the surface of the fin, are solved numerically using the spectral collocation method. The effects of the different parameters as mentioned above are studied with the aid of plotted graphs.

Figure 2 shows the temperature distributions for different values of Nc i.e., the buoyancy parameter. From this plot one can see that as Nc increases the temperature distribution decreases. The effect of the radiation parameter *Nr* on the temperature profile is as shown in Fig.3. Here we can see that as the radiation parameter increases the temperature profile decreases. It proves that the radiation parameter quite effectively controls the temperature, so it has an important role in cooling the system.

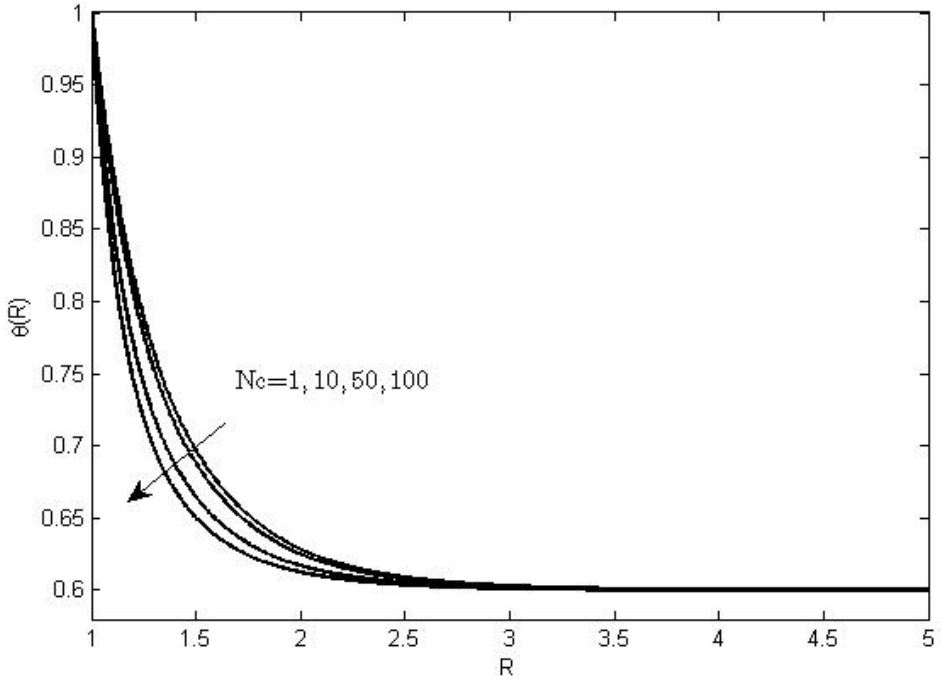

Fig.2. Temperature distributions at $\theta_a = 0.6$, $Nr = 5$, $m = 0.1$, $m_2 = 1$, $p = 2$ and $R^* = 5$, for different values of Nc.

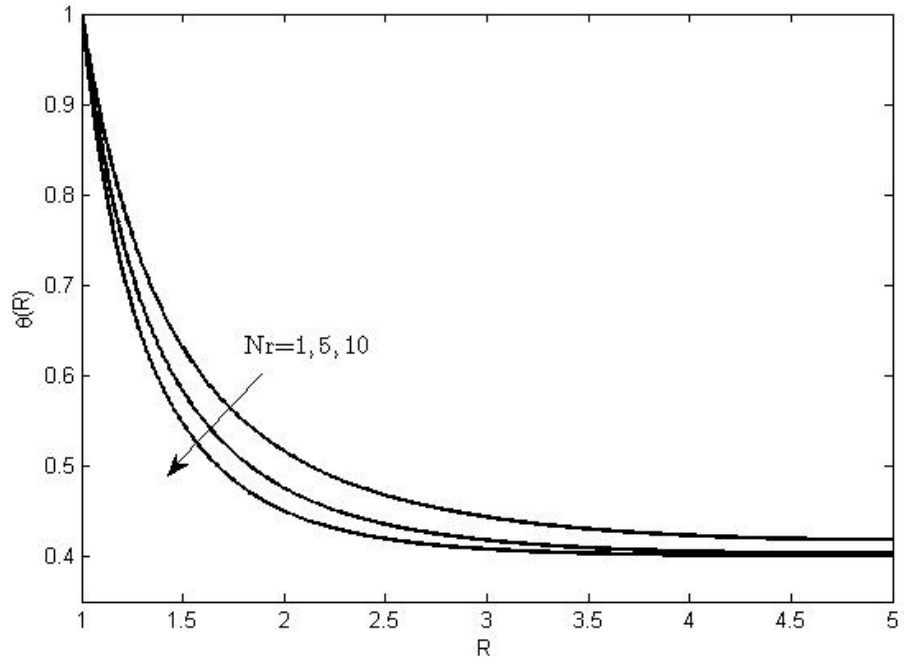

Fig.3. Temperature distributions at $\theta_a = 0.4$, Nc = 10, $m = 1$, $m_2 = 1$, $p = 2$ and $R^* = 5$, for different values of *Nr*.

Figure 4 shows the effect of the dimensionless ambient temperature parameter θ_a on the temperature profile. From this one can realize that as θ_a increases the temperature profile increases. Further observations show that there is a rapid change in the temperature profile with the ambient temperature parameter.

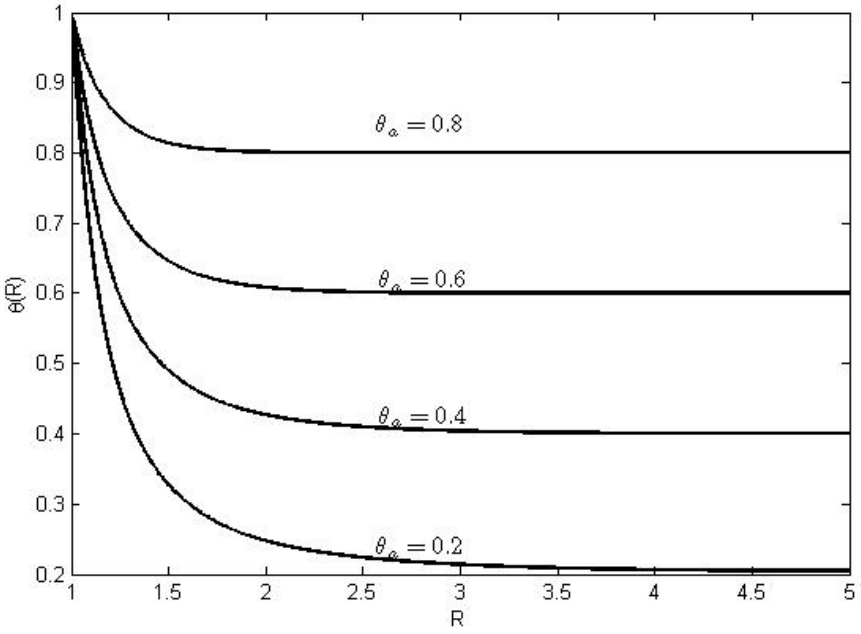

Fig.4. Temperature distributions at $Nr = 10$, Nc = 50, $m = 0$, $m_2 = 0.1$, $p = 1$ and $R^* = 5$, for different values of θ_a.

The role of m_2 on the temperature profile is plotted in Fig.5. It shows that as m_2 increases the temperature profile decreases. Figures 6 and 7 respectively show the importance of the thermal conductivity parameter *m* and *p* on the temperature profile. From this we can see that as *m* and *p* increase the temperature profile also increases. This shows that the thermal conductivity parameter and *p* help in enhancing the temperature profile.

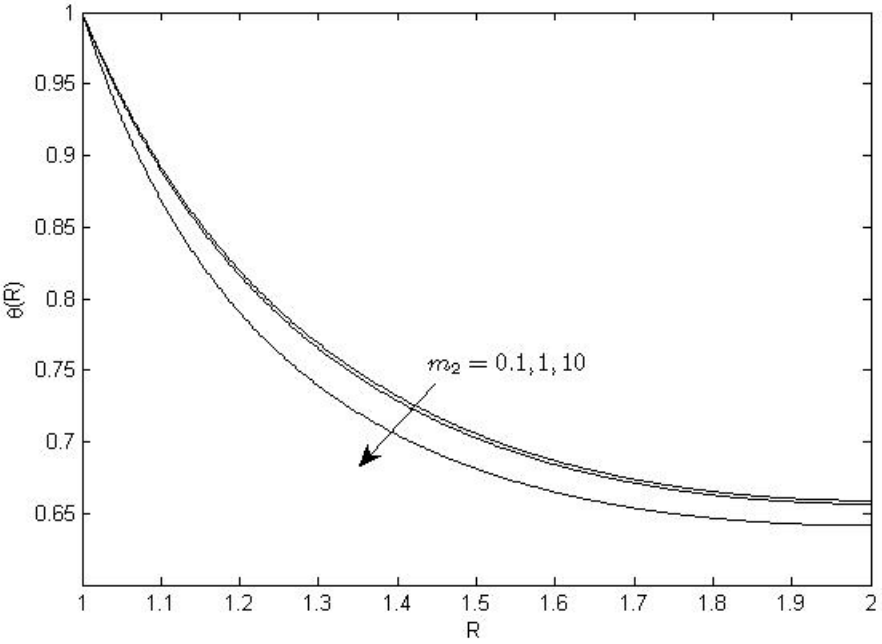

Fig.5. Temperature distributions at $\theta_a = 0.6$, $Nr = 5$, $m = 0.1$, Nc = 1, $p = 1$ and $R^* = 2$, for different values of m_2.

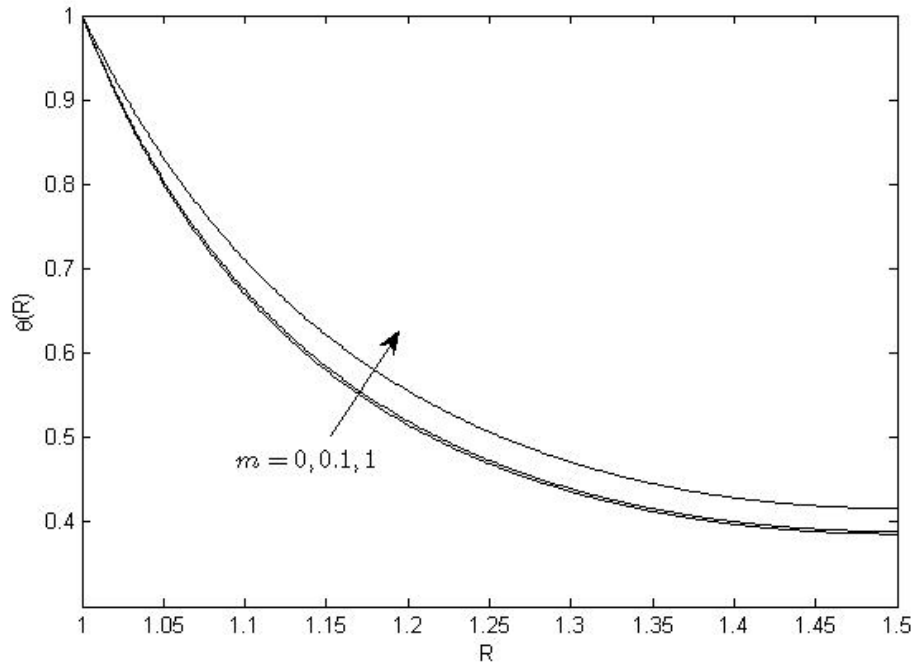

Fig.6. Temperature distributions at $\theta_a = 0.2$, $Nr = 1$, $\mathrm{Nc} = 50$, $m_2 = 10$, $p = 1$ and $R^* = 1.5$, for different values of *m*.

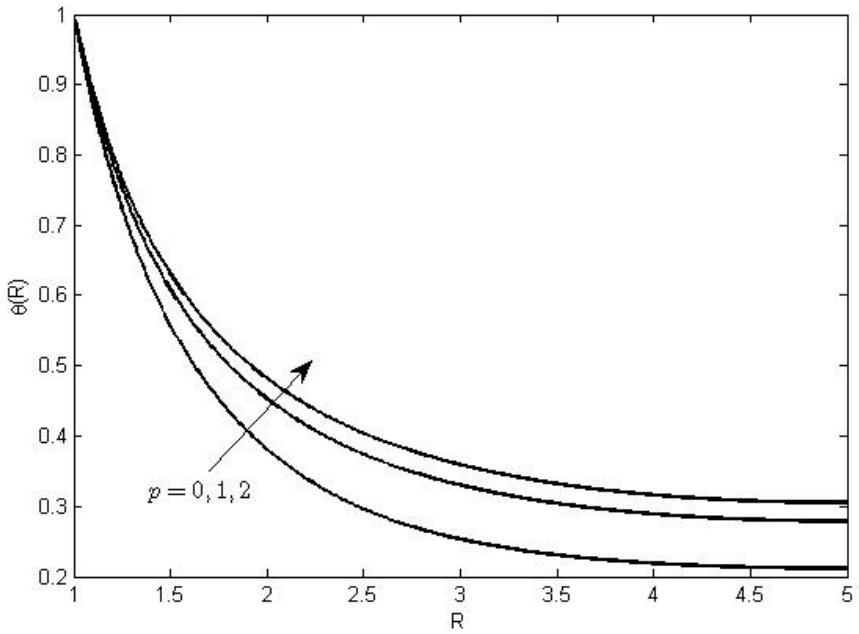

Fig.7. Temperature distributions at $\theta_a = 0.2$, $Nr = 1$, $\mathrm{Nc} = 1$, $m = 0.1$, $m_2 = 1$ and $R^* = 5$, for different values of *p*.

Figure 8 shows the effect of the radiation parameter *Nr* and buoyancy parameter Nc on the dimensionless heat flow. From this figure we can see the rapid increase in dimensionless heat flow for increasing values of Nc and *Nr*. From Fig.9 one can see the role of the ambient fluid temperature θ_a and ratio of tip radius to base radius R^* on the dimensionless heat flow. This figure shows that the dimensionless

heat flow increases with an increase in both the ambient fluid temperature θ_a and the ratio of tip radius to base radius R^*. Further observation shows that as the tip radius of the fin increases the dimensionless heat flow also increases whereas one can find the reverse trend with the base radius of the fin.

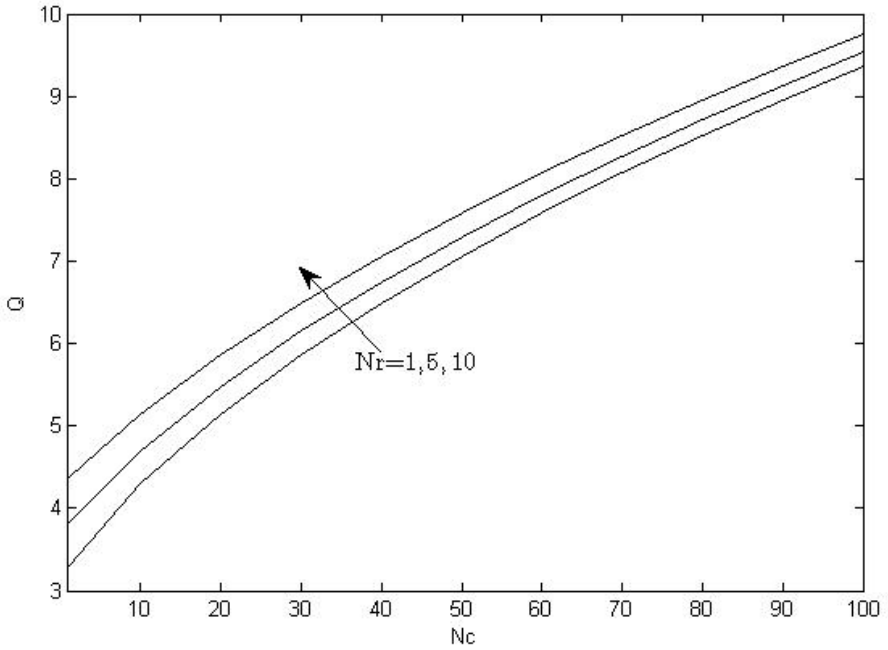

Fig.8. Dimensionless base heat flow: effect of natural convection and radiation when $\theta_a = 0.2, m = 1, m_2 = 10, p = 2, R^* = 5$.

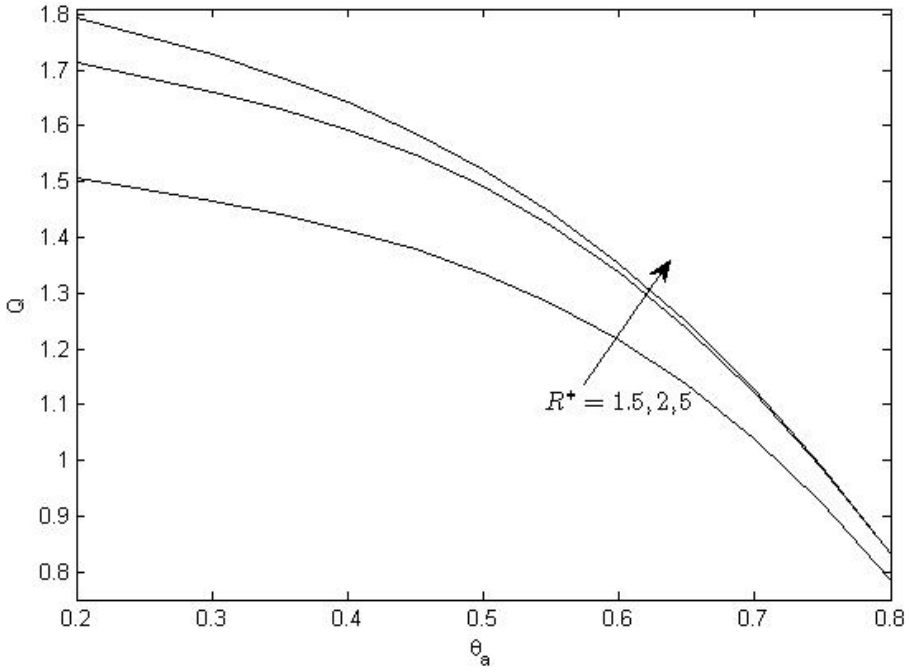

Fig.9. Dimensionless base heat flow: effect of natural convection and ambient temperature when $Nr = 5, \mathrm{Nc} = 1, m = 0.1, m_2 = 10, p = 2$.

The effect of both the ambient fluid temperature θ_a and the radiation parameter *Nr* on the dimensionless heat flow is plotted in Fig.10. It shows that the increasing values of ambient fluid temperature θ_a and radiation parameter *Nr* will enhance the dimensionless heat flow rapidly. A similar effect on dimensionless heat flow can be seen with the combined effects of radiation parameter *Nr* with *p* and m_2 and these are plotted in Figs 11 and 12, respectively.

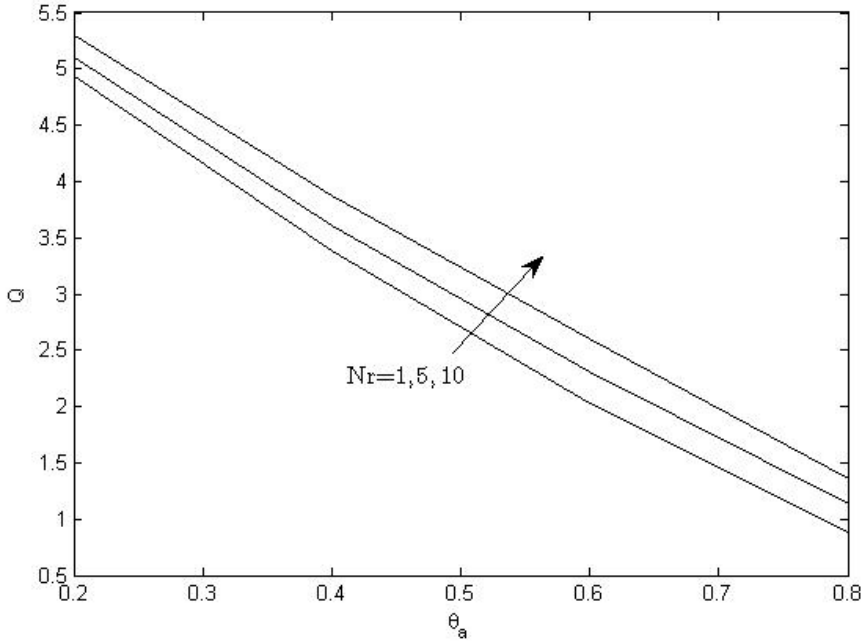

Fig.10. Dimensionless base heat flow: effect of radiationand ambient temperature when $\mathrm{Nc} = 50, m = 0.1, m_2 = 10, p = 1, R^* = 5$.

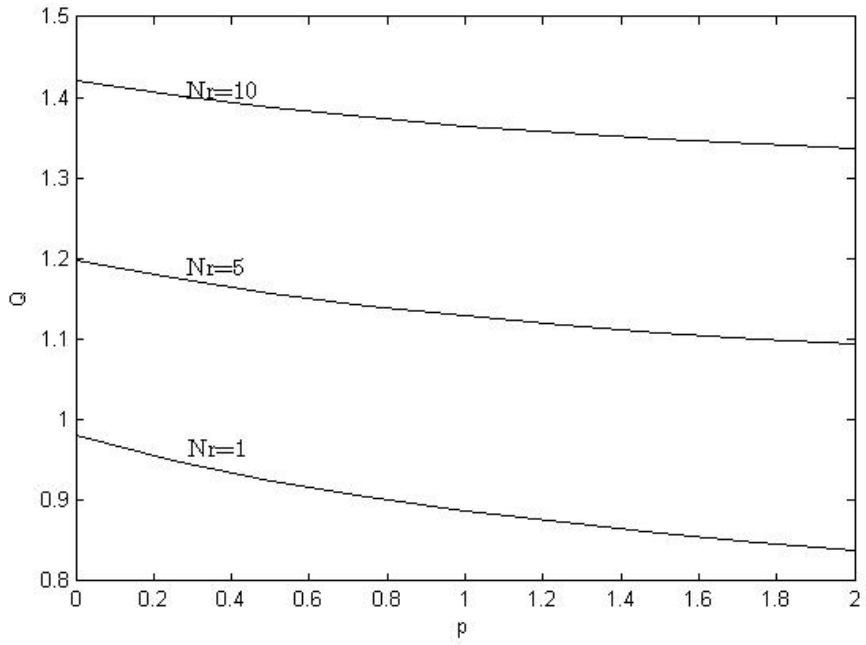

Fig.11. Dimensionless base heat flow: effect of radiation and *p* when $\theta_a = 0.8, \mathrm{Nc} = 50, m = 0.1, m_2 = 10, R^* = 2$

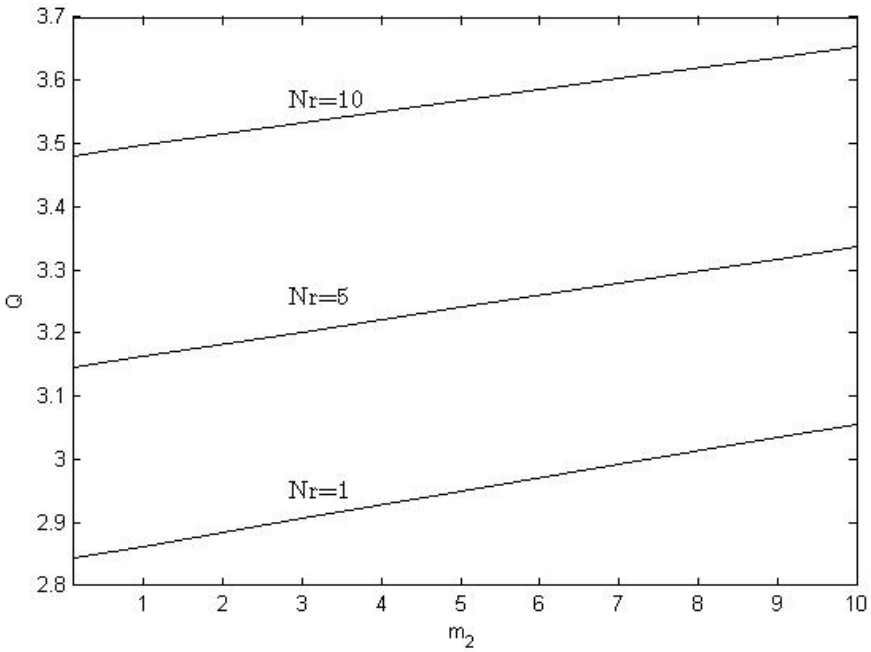

Fig.12. Dimensionless base heat flow: effect of radiation and m_2 when $\theta_a = 0.6, \mathrm{Nc} = 100, m = 1, p = 2, R^* = 2$.

Further, Fig.13 shows the effect of the ratio of tip radius to base radius R^* and p on dimensionless heat flow. From this one can see that dimensionless heat flow increases with an increase in both R^* and p. It shows that as the tip radius of the fin increases, the dimensionless heat flow increases, whereas one can find the reverse trend with the base radius of the fin.

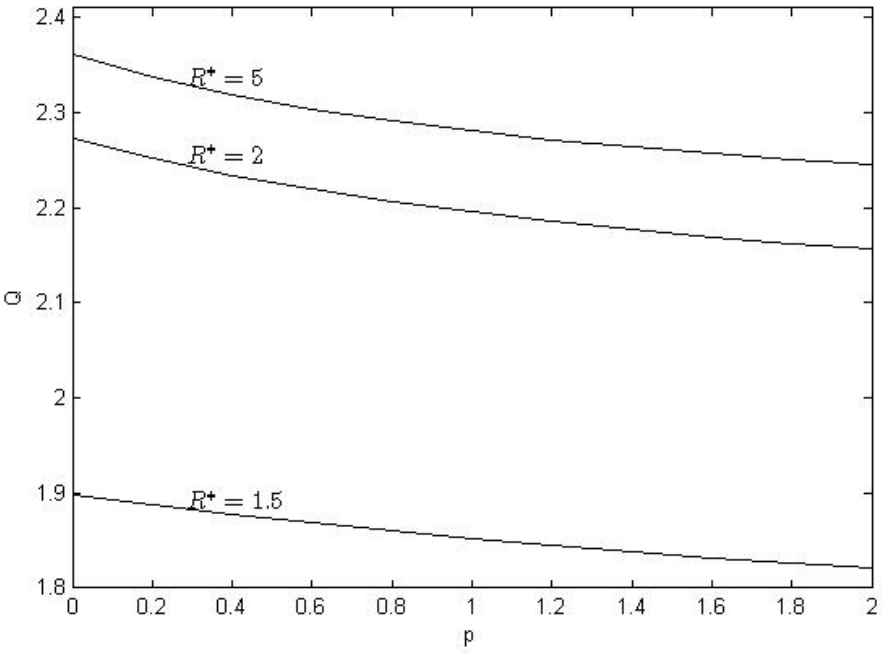

Fig.13. Dimensionless base heat flow: effect of natural convection and p when $\theta_a = 0.4, Nr = 1, \mathrm{Nc} = 10, m = 1, m_2 = 1$.

5. Concluding remarks

A numerical solution for the thermal analysis of a fully wet porous radial fin with natural convection and radiation is obtained with the classic Newton iteration method. The effects of different dimensionless parameters on temperature and dimensionless heat flow are studied with the aid of plotted graphs. Some important findings of the problem are as follows:

- The temperature profiles decrease with increasing values of the buoyancy parameter, radiation parameter, and m_2.
- The effects of the ambient fluid temperature, thermal conductivity parameter, and p are in favor of the temperature profile.
- The combined effects of the radiation parameter with buoyancy parameter, ambient fluid temperature, p, and m_2 are in favor of the dimensionless heat flow.
- The dimensionless heat flow increases with increasing values of the ambient fluid temperature with the ratio of tip radius to base radius and p.
- The dimensionless heat flow increases with increasing values of the tip radius of the fin and decreases with increasing values of the base radius of the fin.

Acknowledgments

The authors are grateful to the reviewers for the constructive remarks.

Nomenclature

$c_{p,f}$ – specific heat of the nambient fluid
D – Chebyshev spectral differentiation matrix
Da – Darcy number
F_{f-a} – shape factor for radiation heat transfer
g – acceleration due to gravity
K_r – thermal conductivity ratio
k – thermal conductivity of ambient fluid
k_{eff} – effective thermal conductivity of porous fin
L – length of the fin
m – thermal conductivity parameter
m_0, m_1, p, $m_2 = m_0 + m_1$ – constants defined in Eq.(2.11)
Nc – Buoyancy or natural convection parameter
Nr – radiation parameter
Q – dimentionless base heat flow
q – base heat flow
R – dimensionless radius
R^* – ratio of tip radius to base radius
r – tadial coordinate
r_b – base radius
r_t – tip radius
T – local fin temperature
T_a – ambient temperature
T_b – base temperature
t – Fin thickness

α_f – thermal diffusivity of ambient fluid
β_f – volumetric thermal expansion coefficient of the ambient fluid
$\in$ – surface emissivity of fin
θ – non-dimensional temperature
θ_a – dimensionless ambient temperature
ρ_f – density of the ambient fluid
σ – Stefan-Boltzmann constant
ν_f – kinematic viscosity of the ambient fluid

References

[1] Nguyen A. and Aziz A. (1992): *The heat transfer rate from convecting-radiating fins for different profile shapes*. – Heat and Mass Transfer, vol.27, pp.67-72.

[2] Yu L.T. and Chen C.K. (1999): *Optimization of circular fins with variable thermal parameters*. – J. Franklin Institute, vol.336, pp.77-95.

[3] Abu-Hijleh (2003): *Enhanced forced convection heat transfer from a cylinder using permeable fins*. – ASME J. Heat Transfer, vol.125, pp.804-811.

[4] Kiwan S. (2006): *Thermal analysis of natural convection in porous fins*. – Transport in Porous Media, vol.67, pp.17-29.

[5] Mobedi M. and Sunden B. (2006): *Natural convection heat transfer from a thermal heat source located in a vertical plate fin*. – Int. J. Heat Mass Transfer, vol.33, pp.943-950.

[6] Lorenzini G. and Moretti S. (2007): *Numerical analysis on heat removal from Y-shaped fins: efficiency and volume occupied for a new approach to performance optimization*. – Int. J. Thermal Science, vol.46, pp.573-579.

[7] Kundu B. and Bhanja D. (2010): *Performance and optimization analysis of a constructal T-shaped fin subject to variable thermal conductivity and convective heat transfer coefficient*. – Int. J. Heat Mass Transfer, vol.53, pp.254-267.

[8] Khani F. and Abdul Aziz (2010*): Thermal analysis of a longitudinal trapezoidal fin with temperature-dependent thermal conductivity and heat transfer coefficient*. – Commun Nonlinear Sci Numer Simulat, vol.15, pp.590–601.

[9] Turkyilmazoglu M. (2012): *Exact solutions to heat transfer in straight fins of varying exponential shape having temperature dependent properties*. – International Journal of Thermal Sciences, vol.55, pp.69-75.

[10] Gorla R.S.R. and Bakier A.Y. (2011): *Thermal analysis of natural convection and radiation in porous fins*. – Int. Commun. Heat Mass Transfer, vol.38, pp.638-645.

[11] Turkyilmazoglu M. *Exact heat-transfer solutions to radial fins of general profile*. – Journal of Thermophysics and Heat Transfer, DOI: 10.2514/1.T4555.

[12] Masoud Asadi1 and Ramin Haghighi Khoshkho (2013): *Temperature distribution along a constant cross sectional area fin*. – Int. Jou. of Mech. and App., vol.3, No.5, pp.131-137.

[13] Hatami M. and Ganj D.D. (2013): *Thermal performance of circular convective–radiative porous fins with different section shapes and materials*. – Energy Conversion and Management, vol.76, pp.185–193.

[14] Hafiz Muhammad Ali and Muhammad Abubaker (2014): *Effect of vapour velocity on condensate retention on horizontal pin-fin tubes*. – Energy Conversion and Management, vol.86, pp.1001–1009.

[15] Erdem Cuce and Pinar Mert Cuce (2015): *A successful application of homotopy perturbation method for efficiency and effectiveness assessment of longitudinal porous fins*. – Energy Conversion and Management, vol.93, pp.92–99.

[16] Turkyilmazoglu M. (2015): *Stretching/shrinking longitudinal fins of rectangular profile and heat transfer*. – Energy Conversion and Management, vol.91, pp.199–203.

[17] Darvishi M.T. (2007): *Spectral collocation method and Darvishis preconditionings for Tchebychev-Gauss-Lobatto points*. – International Mathematical Forum, vol.2, No.6, pp.263–272.

[18] Canuto C., Hussaini M.Y., Quarteroni A. and Zang T.A. (2006): *Spectral Methods: Fundamentals in Single Domains*. – Berlin: Springer.

[19] Subich C.J., Lamb K.G. and Stastna M. (2013): *Simulation of the Naviere-Stokes equations in three dimensions with a spectral collocation method*. – Int. J. Numer. Methods Fluids, vol.73, pp.103-129.

[20] Li B.W., Zhao Y.R. and Yu Y. (2011): *Three-dimensional transient Naviere-Stokes solvers in cylindrical coordinate system based on a spectral collocation method using explicit treatment of the pressure*. – Int. J. Numer. Methods Fluids, vol.66, pp.284-298.

[21] Abbasbandy S., Ghehsareh H.R. and Hashim I. (2012): *An approximate solution of the MHD flow over a non-linear sheet by rational chebyshev collocation method*. – Sci. Bull. A, vol.74, pp.47-58.

[22] Darvishi M.T., Khani F. and Abdul Aziz (2015): *Numerical investigation for a hyperbolic annular fin with temperature dependent thermal conductivity*. – Propulsion and Power Research, (accepted)

Received: September 27, 2015

Revised: March 18, 2016